GEOPHYSICS, VOL. 67, NO. 3 (MAY-JUNE 2002); P. 883–889, 8 FIGS.
10.1190/1.1484531

Offset and angle-domain common image-point gathers for shot-profile migration

James E. Rickett* and Paul C. Sava‡

ABSTRACT

Prestack depth migration of shot profiles by downward continuation is a practical imaging algorithm that is especially cost-effective for sparse-shot wide-azimuth geometries. The interpretation of offset as the displacement between the downward-propagating (shot) wavefield and upward-propagating (receiver) wavefield enables us to extract offset-domain common image-point (CIP) gathers during shot-profile migration. The offset-domain gathers can then be transformed to the angle domain with a radial-trace mapping originally introduced for shot-geophone migration. The computational implications of this procedure include both the additional cost of multioffset imaging and an implicit transformation from shot-geophone to midpoint-offset coordinates. Although this algorithm provides a mechanism for imaging angle-dependent reflectivity via shot-profile migration, for sparse-shot geometries the fundamental problem of shot-aliasing may severely impact the quality of CIP gathers.

INTRODUCTION

Driven by the dramatic decrease in the cost of computer power, geophysicists are becoming increasingly interested in "wave-equation" migration algorithms based on downward continuation as an alternative to Kirchhoff methods for 3-D prestack depth migration. Wave-equation methods naturally model the finite-frequency effects of wave propagation such as multipathing that can cause problems in structurally complex areas.

Two popular algorithms for prestack imaging by downward continuation are *shot-geophone* migration and *shot-profile* migration. Shot-geophone migration is based on the concept of survey-sinking (Claerbout, 1985); the entire wavefield is extrapolated at once with the double square-root (DSR) equation (Claerbout, 1985), and the image is extracted at zero-offset and zero-time. In contrast, during shot-profile migration, the upgoing and downgoing wavefields are extrapolated separately with the single square-root equation. The image is then extracted by crosscorrelating the two wavefields and summing over frequency to invoke the zero-time imaging condition (Claerbout, 1971). The final image is then obtained by summing over shots. The process of imaging in this way can be described by the equation

$$I(\mathbf{x}, z) = \sum_s \sum_\omega q_-(\mathbf{x}, z, \omega, s)\, q_+(\mathbf{x}, z, \omega, s)^*, \qquad (1)$$

where the image, $I(\mathbf{x}, z)$, is a function of midpoint and depth, q_- and q_+ represent the downward and upward propagating wavefields, respectively, s is the shot index, and ω denotes temporal frequency.

For shot-geophone migration in midpoint-offset coordinates, the cost of extrapolating a single-depth step with a basic split-step extrapolator (Stoffa et al., 1990) is proportional to $N_{xy} N_{hxy} \log(N_{xy} N_{hxy})$, where N_{xy} is the number of midpoints and N_{hxy} is the number of offsets. The analogous cost for shot-profile migration is proportional to $N_{xy} N_{sxy} \log(N_{xy})$, where N_{sxy} is the number of shots, because although the wavefield is not a function of offset, each shot must be migrated separately.

Therefore, for geometries with large numbers of shots (such as typical 3-D marine streamer geometries), shot-geophone migration is a more attractive choice, especially when the dimensionality of the problem can be reduced by common-azimuth (Biondi and Palacharla, 1996) or offset-plane wave (Mosher et al., 1997) approximations. However, for wide-azimuth geometries where the number of shots (or receivers in the reciprocal sense) is small compared to the number of offsets,

Presented at the 71st Annual International Meeting, Society of Exploration Geophysicists. Manuscript received by the Editor June 1, 2001; revised manuscript received November 13, 2001.
*Formerly Stanford Exploration Project, Department of Geophysics, Stanford University, Stanford, California 94583-2324; presently Chevron Texaco Exploration and Production Technology Company, 6001 Bollinger Canyon Road, San Ramon, California 94583-2324. E-mail: JamesRickett@ChevronTexaco.com.
‡Stanford Exploration Project, Mitchell Building, Department of Geophysics, Stanford University, Stanford, California 94305-2215. E-mail: paul@sep.Stanford.edu.

shot-profile migration may be preferable. Three-dimensional data collected with technologies such as vertical cables, borehole seismometers, and ocean bottom seismometers may be efficiently migrated with shot-profile methods [e.g., Anderson et al. (1997); Purnell et al. (2000)]. Furthermore, shot-profile migration may be made even more cost-competitive if other computational tricks are employed, such as the phase-encoding of shot gathers (Romero et al., 2000).

An often-perceived disadvantage of shot-profile migration, however, is the difficulty in obtaining common image-point (CIP) gathers that can be used for velocity analysis and/or amplitude variation with offset (AVO) studies. While both velocity and AVO analyses are often performed in the common midpoint domain, studies indicate that there are significant advantages to performing them in the CIP domain after migration. For example, both simple vertical updating with the Deregowski loop (1990) and state-of-the-art reflection tomography [e.g., Stork (1992); Clapp (2001)] necessarily requires prestack migrated data. With regard to amplitude analysis, Mosher et al. (1996) reviews several case studies where migration significantly improves the reliability of AVO attribute maps.

In this paper, we describe a new approach for extracting angle-domain CIP gathers during shot-profile migration. We interpret offset as the lateral displacement between upgoing and downgoing wavefields. Rather than extracting a single image at zero-time, we extract multiple nonzero offset images, allowing us to form offset-domain CIP gathers. These offset-domain CIP gathers may then be converted to angle-domain gathers with Sava and Fomel's (2000) radial-trace transformation. The algorithm compares favorably with de Bruin et al.'s (1990) approach, which images offset-ray parameter gathers with a slant stack as part of the imaging step.

We discuss the additional cost of multioffset imaging, and the implications of the implicit transformation from shot-geophone to midpoint-offset coordinates. We also demonstrate that although the algorithms exist for imaging angle-dependent reflectivity with shot-profile migration, the sparse-shot geometries, to which these methods are best suited, suffer from the fundamental problem of shot aliasing. Shot aliasing is an inherent feature of sparse-shot geometries and may require regularized least-squares migration (Ronen and Liner, 2000) to solve.

ANGLE-DEPENDENT IMAGING AFTER MIGRATION

De Bruin et al. (1990) first described a method for calculating angle-dependent reflectivity with a wave-equation migration process. Their algorithm is appropriate for shot-profile migrations and involves forming offset-ray parameter gathers with a local slant stack as part of the image-forming step.

Similarly, Prucha et al. (1999) describe how to extract offset-ray parameter gathers with a slant stack during shot-geophone migration in the offset-midpoint domain. The offset-ray parameter ($\mathbf{p}_h$) axes can be related to incidence angle at the reflector (γ) by the trigonometric formula,

$$\mathbf{p}_h = \begin{pmatrix} p_{h_x} \\ p_{h_y} \end{pmatrix} = \frac{2 \sin\gamma \cos\theta}{v_{\text{int}}(\mathbf{x}, z)} \begin{pmatrix} \cos\phi \\ \sin\phi \end{pmatrix}, \tag{2}$$

where θ is the reflector dip, ϕ is the azimuth of the maximum down-dip direction measured counter clockwise from the x-axis, and v_{int} is the interval velocity.

For shot-geophone migration in offset-midpoint coordinates, Sava and Fomel (2000) provide an algorithm that converts offset-domain CIP gathers to the angle domain, Their transformation is a radial-trace mapping in the offset-depth wavenumber ($\mathbf{k}_h, k_z$) domain, based on the relation

$$\tan\gamma = -\left.\frac{\partial z}{\partial h}\right|_{t,\mathbf{x}} = -\frac{|\mathbf{k}_h|}{k_z}, \tag{3}$$

where $h = \sqrt{h_x^2 + h_y^2}$ is the magnitude of the half-offset vector $\mathbf{h}$. The imaging condition ($t = 0$) provides the constant t, and the common midpoint nature of CIP gathers provides the constant $\mathbf{x}$ required by the partial derivative. Appendix A reviews a derivation of equation (3) and briefly describes the practical implementation of this transformation.

Sava and Fomel's (2000) formulation has the advantage over Prucha et al.'s (1999) approach in that the transformation to the angle domain is independent of both the reflector dip and interval velocity. Equation (3) maps offset-domain gathers directly to the angle domain with no need for equation (2).

Offset in shot-profile migration

To understand how to obtain offset-domain CIP gathers after shot-profile migration, it is first necessary to understand that the downward continuation process changes the effective offset of energy in the seismic wavefield. After wave-equation migration, offset no longer refers to the recording offset at the surface, but rather refers to the effective subsurface offset between upgoing and downgoing wavefields. Offset after migration is therefore a model-space rather than a data-space parameter. Figure 1 graphically illustrates the different meaning of offset before, during, and after migration by downward continuation.

Although shot-geophone migration can be performed with an explicit offset axis, it is less apparent what offset means for the case of shot-profile migration. We interpret offset as the displacement between the downward-going (shot) and upward-going (receiver) wavefields. Rather than extracting a single zero-offset/zero-time reflectivity image with equation (1), we can extract an image that contains multiple offsets through the equation

$$I(\mathbf{x}, \mathbf{h}, z) = \sum_s \sum_\omega q_-(\mathbf{x} - \mathbf{h}, z, \omega, s)\, q_+(\mathbf{x} + \mathbf{h}, z, \omega, s)^*. \tag{4}$$

The concept of multioffset imaging via equation (4) is compatible with deconvolution imaging conditions such as the U/D (upward over downward) approach originally proposed by Claerbout (1971).

The migration procedure follows closely the conventional shot-profile imaging methodology. The source and receiver wavefields are extrapolated separately into the earth. At each depth step, the imaging is performed with equation (4) to produce CIP gathers that are functions of depth, offset, and midpoint.

Gathers produced this way contain off-diagonal elements of Berkhout's (1985) reflectivity matrix and are equivalent to those produced by imaging multiple nonzero offsets in an offset-midpoint shot-geophone migration. Consequently, the offset axes can be mapped to angle with Sava and Fomel's (2000) transformation described in equation (3).

NUMERICAL CONSIDERATIONS

Shot-to-midpoint transformation

Implicit in the multioffset imaging scheme outlined above is a transformation from shot-receiver to midpoint-offset space. Although this transformation is buried within the migration process, the subtleties associated with the conversion remain.

If the wavefields are sampled with spacing Δx, then equation (4) will image with half-offset spacing $\Delta h = \Delta x$, as shown in Figure 2a. Sampling in offset can be refined further by considering Figure 2b; however, to do so requires imaging onto midpoints which do not lie on the propagation grid.

This problem is experienced whenever data are transformed from shot-geophone to midpoint-offset space, and no perfect solution exists. A typical workaround is to refine the midpoint grid and fill empty bins with zeros; however, this doubles the data volume and hence also doubles the cost of migration. Another alternative is to process even and odd offset separately; the disadvantage of this approach is that each half of the data set may be undersampled.

Since shot-profile migration works in the shot-geophone domain, these problems may be avoided until after the migration is complete. Migration decreases the data volume, increases the signal-to-noise ratio, and resolves locally conflicting dips. Therefore, it is easier to resample the data on whatever grid suits the interpreter after migration.

Computational cost

As discussed in the introduction, the cost of downward continuing a 3-D wavefield one depth step in the Fourier domain is proportional to $N_{xy}\log(N_{xy})$. On the other hand, the cost of imaging with equation (4) is proportional to $N_{xy}N_{h_{xy}}$. Clearly, if the number of offsets is large, then the cost of the imaging step may be comparable (or even greater) than the cost of the downward continuation. However, this additional cost is not as serious a problem as it first appears.

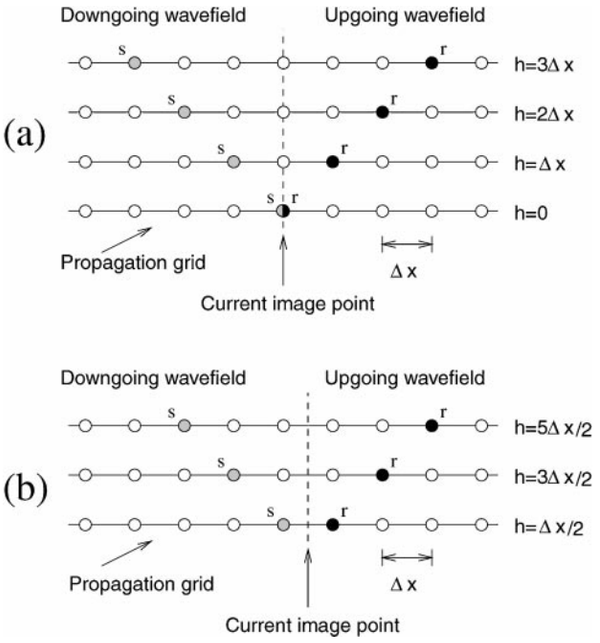

FIG. 2. Midpoint-offset sampling during migration. Panel (a) shows imaging offsets with $\Delta h = \Delta x$ based on equation (4) alone. Panel (b) shows the additional offsets that are imaged with $\Delta h = \Delta x/2$. The midpoints in this panel lie between propagation grid nodes.

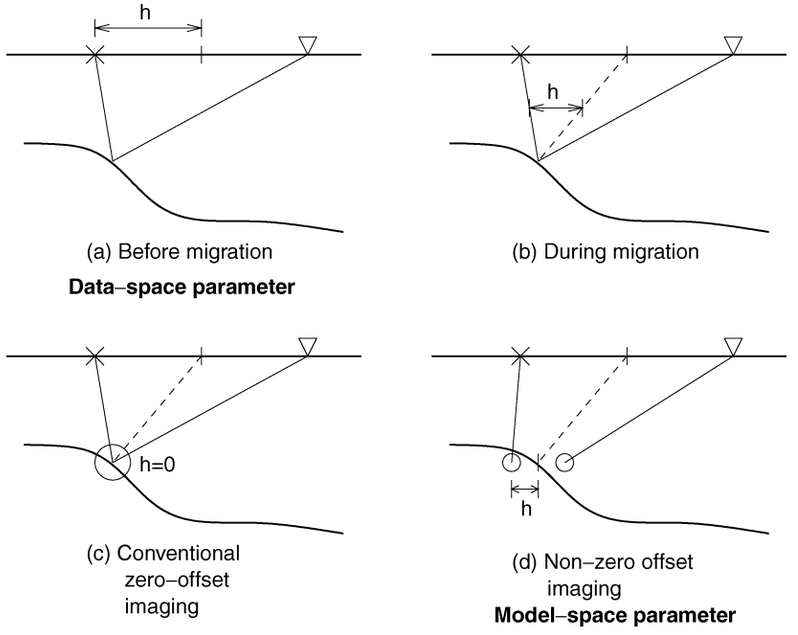

FIG. 1. Illustration of how the effective offset of specular energy changes as the wavefield is downward continued into the earth. Panels show offset before (a), during (b), and after (c, d) migration.

Since the effective offset is focused towards zero by the imaging process, only a narrow range of offsets near zero are usually needed to capture the angle-dependent reflectivity adequately.

The additional cost of nonzero offset imaging that comes with equation (4) comes from the fact that the imaging step must be repeated for each shot profile. Phase encoding of shots (Romero et al., 2000) allows many shots to be migrated simultaneously and is fully compatible with multioffset imaging as described in this paper. Combining the two methodologies will facilitate rapid angle-dependent imaging via shot-profile migration.

The increase in computational cost associated with imaging is never a problem with shot-geophone migration. With it, the cost of the imaging step (proportional to $N_{xy}N_{hxy}$), is always less than the cost of the downward continuation [proportional to $N_{xy}N_{hxy}\log(N_{xy}N_{hxy})$].

INTERPRETATION OF CIP GATHERS

Effect of velocity on common-image gathers

Figure 3 illustrates the effect velocity plays on offset-domain common-image gathers. The three panels show CIP gathers produced by migrating the Marmousi (Bourgeois et al., 1991) synthetic data set with three different velocity models: the correct velocity [panel (a)], a velocity that is too high [panel (b)], and a velocity model that is too low [panel (c)]. Interpreting patterns in the offset-domain CIP gathers is difficult; however, after transformation to the angle domain (Figure 4), standard residual-moveout patterns indicate the sign of the

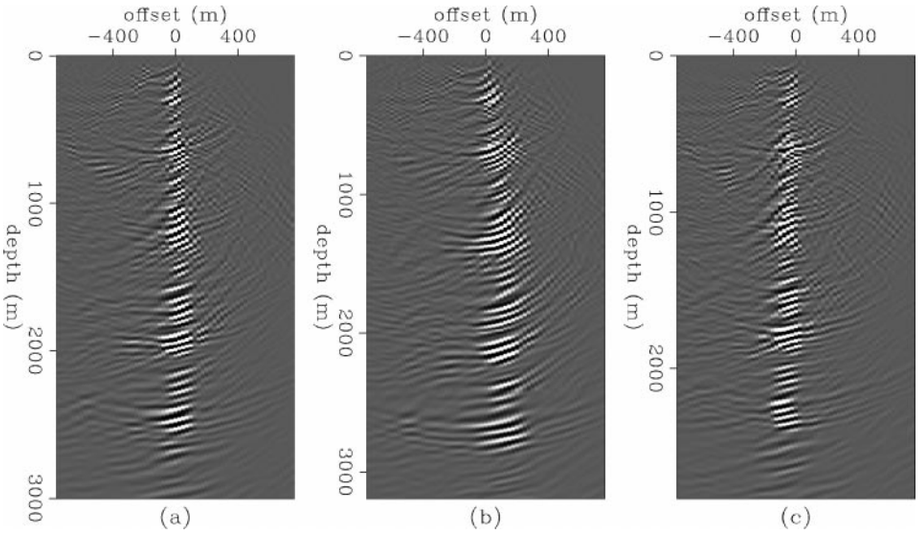

FIG. 3. Offset-domain common-image gathers corresponding to $x = 4000$ m. Panels (a), (b), and (c) were migrated with velocity models that were correct, 6% too high, and 6% too low, respectively.

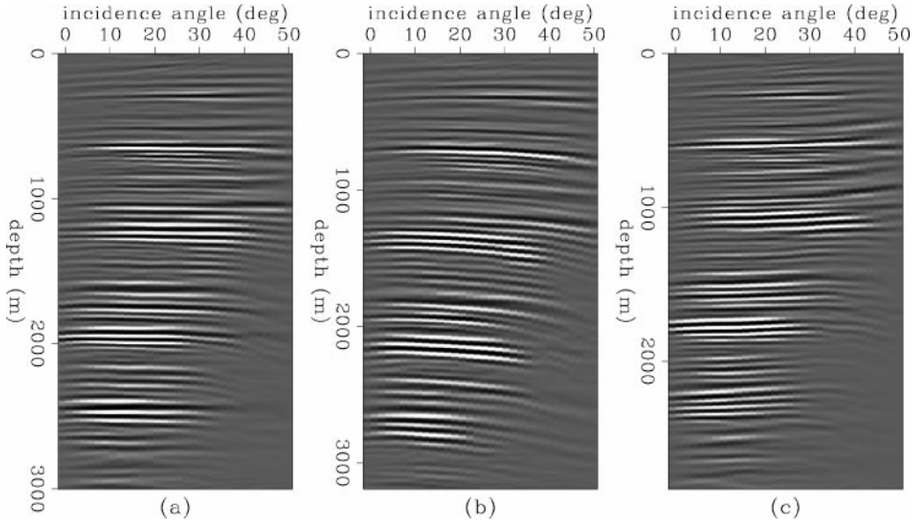

FIG. 4. Angle-domain common-image gathers corresponding to $x = 4000$ m. Panels (a), (b), and (c) were migrated with velocity models that were correct, too high, and too low, respectively.

velocity error: events curving up means too low, and events curving down means too high.

Effect of shot sampling on common-image gathers

As discussed previously, data sets collected with sparse-shot geometries are most suitable for shot-profile migration. Figure 5 compares the migrated (zero-offset) images of the two prestack data sets. The data set that produced panel (a) had a fully-sampled shot axis, whereas the shot axis on the data set that produced panel (b) contained only every 20th shot. Even with the very sparsely sampled shot axis, the geologic structure is clearly interpretable in Figure 5b.

To illustrate the problems associated with sampling for shot-profile migrations, Figure 6 shows the same image gathers as Figure 3, but after migrating only every 20th shot. Energy is no longer concentrated around zero offset. Figure 7a shows the equivalent picture in the angle domain. Although the velocity is correct and the zero-offset image [Figure 5b] seems reasonable, coverage in the angle domain is very irregular. When the velocities are incorrect, the angle gathers remain chaotic: shot aliasing has effectively rendered the angle-gathers uninterpretable in terms of velocities.

Although both de Bruin et al.'s (1990) original methodology and the approach described here provide means of obtaining CIP gathers from shot-profile migration, the problem of shot aliasing remains important for the geometries that are best suited to shot-profile migration. A potential solution to this problem lies in regularized least-squares migration because this can overcome conventional aliasing criteria [see Ronen and Liner (2000) for a review]. However, iterative least-squares migration is both expensive and very sensitive to the inversion parameters. Least-squares wave-equation depth migration [e.g., Prucha et al. (2000)] is very much a research topic.

CONCLUSIONS

We construct offset-domain CIP gathers after shot-profile migration by interpreting offset as the displacement between upgoing and downgoing wavefields. The offset-domain gathers then can be transformed to the angle domain by Sava and Fomel's (2000) transformation where residual moveout can be used for residual velocity analysis or image enhancement. The

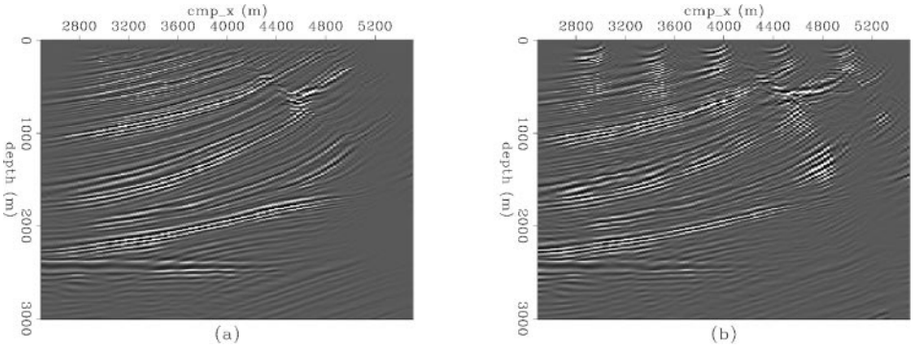

FIG. 5. Migrated images produced with data having a fully-sampled shot axis (a), and a very sparsely sampled shot axis (b).

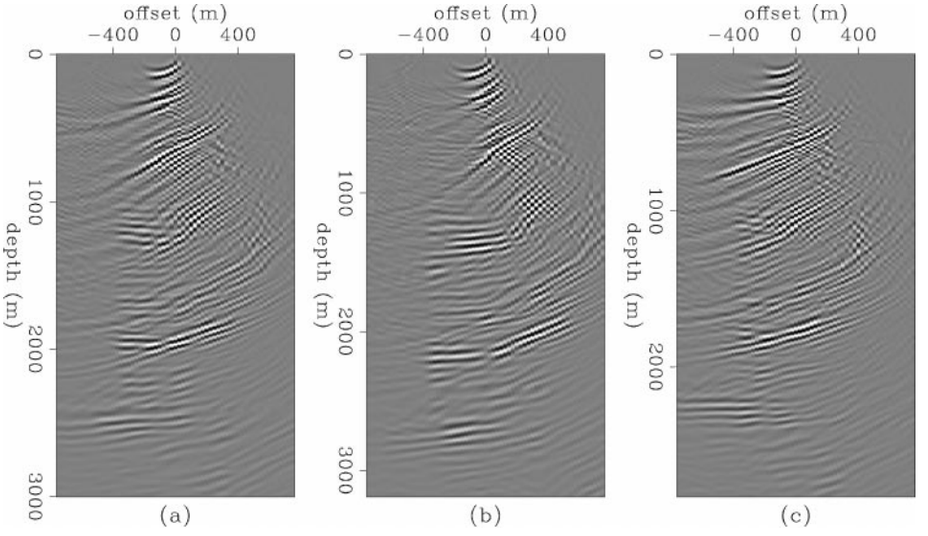

FIG. 6. Poorly illuminated offset-domain common-image gathers corresponding to $x = 4000$ m. Panels (a), (b), and (c) were migrated with velocity models that were correct, 6% too high, and 6% too low, respectively. Shot spacing was 500 m, instead of 25 m as in Figure 3.

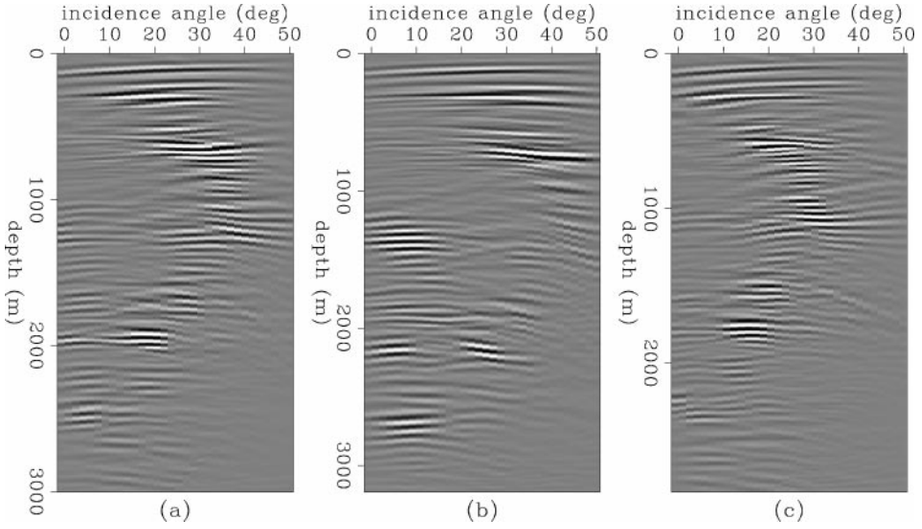

FIG. 7. Poorly illuminated angle-domain common-image gathers corresponding to $x = 4000$ m. Panels (a), (b), and (c) were migrated with velocity models that were correct, 6% too high, and 6% too low, respectively.

angle domain also potentially contains information about reflectivity as a function of angle that may be used to infer rock properties across the reflecting interface.

For sparse-shot geometries suitable for shot-profile migration, however, the problem of shot aliasing remains. Shot aliasing can cause corruption of the angle-domain gather, rendering simple moveout-based velocity analysis very difficult.

REFERENCES

Anderson, J., Noponen, I., Cai, W., Delome, H., Sukup, D., and Boyd, S., 1997, 3-D vertical cable processing to obtain a pre-stack depth-migrated image: 67th Ann. Internat. Mtg., Soc. Expl. Geophys., Expanded Abstracts, 1399–1401.

Berkhout, A. J., 1985, Seismic migration: Elsevier Science Publ. Co.

Biondi, B., and Palacharla, G., 1996, 3-D prestack migration of common-azimuth data: Geophysics, **61**, 1822–1832.

Bourgeois, A., Bourget, M., Lailly, P., Poulet, M., Ricarte, P., and Versteeg, R., 1991, Marmousi, model and data: The Marmousi experience: Proc. of 1990 EAEG workshop on practical aspects of seismic data inversion.

Claerbout, J. F., 1971, Toward a unified theory of reflector mapping: Geophysics, **36**, 467–481.

——— 1985, Imaging the earth's interior: Blackwell Scientific Publications, Inc.

Clapp, R. G., 2001, Geologically constrained migration velocity analysis: Ph.D. thesis, Stanford Univ.

de Bruin, C. G. M., Wapenaar, C. P. A., and Berkhout, A. J., 1990, Angle-dependent reflectivity by means of prestack migration: Geophysics, **55**, 1223–1234.

Deregowski, S. M., 1990, Common-offset migrations and velocity analysis: First Break, **8**, 224–234.

Fomel, S., 1997, Migration and velocity analysis by velocity continuation: Stanford Exploration Project Report **92**, 159–188.

Mosher, C. C., Foster, D. J., and Hassanzadeh, S., 1997, Common angle imaging with offset plane waves: 67th Ann. Internat. Mtg., Soc. Expl. Geophys., Expanded Abstracts, 1379–1382.

Mosher, C. C., Keho, T. H., Weglein, A. B., and Foster, D. J., 1996, The impact of migration on AVO: Geophysics, **61**, 1603–1615.

Prucha, M., Biondi, B., and Symes, W., 1999, Angle-domain common image gathers by wave-equation migration: 69th Ann. Internat. Mtg., Soc., Expl. Geophys., Expanded Abstracts, 824–827.

Prucha, M. L., Clapp, R. G., and Biondi, B., 2000, Seismic image regularization in the reflection angle domain: Stanford Exploration Project Report **103**, 109–119.

Purnell, G., Sukup, D., Higginbotham, J., and Ebrom, D., 2000, Migrating sparse-receiver data for AVO analysis at Teal South field: 70th Ann. Internat. Mtg., Soc. Expl. Geophys., Expanded Abstracts, 1399–1401.

Romero, L. A., Ghiglia, D. C., Ober, C. C., and Morton, S. A., 2000, Phase encoding of shot records in prestack migration: Geophysics, **65**, 426–436.

Ronen, S., and Liner, C. L., 2000, Least-squares DMO and migration: Geophysics, **65**, 1364–1371.

Sava, P., and Fomel, S., 2000, Angle-gathers by Fourier transform: Stanford Exploration Project Report **103**, 119–130.

Sava, P., Fomel, S., and Biondi, B., 2001, Amplitude-preserved common-image gathers by wave-equation migration: 71st Ann. Internat. Mtg., Soc. Expl. Geophys., Expanded Abstracts, 296–299.

Stoffa, P. L., Fokkema, J. T., de Luna Freire, R. M., and Kessinger, W. P., 1990, Split-step Fourier migration: Geophysics, **55**, 410–421.

Stork, C., 1992, Reflection tomography in the postmigrated domain: Geophysics, **57**, 680–692.

APPENDIX A

REVIEW OF OFFSET-DOMAIN TO ANGLE-DOMAIN TRANSFORMATION

In this appendix, we review the theory behind the transformation from offset-domain CIP gathers to the angle domain. The derivation of equation (A-9) given below follows Fomel (1997), and Sava and Fomel (2000) first described its implementation via equation (A-10).

Figure A-1 shows the path specular energy travels as it is downward-continued into the earth during prestack migration. As illustrated in Figure A-1b, we can consider the horizontal locations of the shot and receiver wavepaths at a small vertical distance z above the reflection point as s and r, respectively.

If the velocity is smooth in the vicinity of the reflector, the partial derivatives of traveltime t from s to r with respect to s and r are given by

$$\frac{\partial t}{\partial s} = \frac{\sin\alpha_1}{v} \tag{A-1}$$

and

$$\frac{\partial t}{\partial r} = \frac{\sin\alpha_2}{v}, \tag{A-2}$$

where α_1 and α_2 describe the propagation directions of the source and receiver wavefields, respectively. Defining $x=(r+s)/2$ and $h=(r-s)/2$ and applying the chain rule gives

$$\frac{\partial t}{\partial h} = \frac{\sin\alpha_2}{v} - \frac{\sin\alpha_1}{v} \tag{A-3}$$

$$= \frac{2}{v}\cos\left(\frac{\alpha_2+\alpha_1}{2}\right)\sin\left(\frac{\alpha_2-\alpha_1}{2}\right). \tag{A-4}$$

Identifying $(\alpha_2+\alpha_1)/2$ as the dip angle in the plane of the reflecting energy α, and $(\alpha_2-\alpha_1)/2$ as the opening angle γ leads to the equation,

$$\frac{\partial t}{\partial h} = \frac{2}{v}\cos\alpha\sin\gamma. \tag{A-5}$$

Similar consideration of the partial derivative of traveltime with respect to the change in position of the image point gives

$$-\frac{\partial t}{\partial z} = \frac{\cos\alpha_1}{v} + \frac{\cos\alpha_2}{v} \tag{A-6}$$

$$= \frac{2}{v}\cos\left(\frac{\alpha_2+\alpha_1}{2}\right)\cos\left(\frac{\alpha_2-\alpha_1}{2}\right) \tag{A-7}$$

$$= \frac{2}{v}\cos\alpha\cos\gamma. \tag{A-8}$$

Finally, combining equations (A-5) and (A-8) gives the exact, velocity-independent relationship for the opening angle, γ, which is the basis for the transformation,

$$\tan\gamma = -\frac{\partial z}{\partial h}. \tag{A-9}$$

Sava and Fomel (2000) noticed that equation (A-9) allows you to compute the energy incident at a particular angle by performing a local slant stack in depth-offset CIP gathers. This is subject to a constant velocity assumption along the trajectory of the slant stack. They also observed that this slant stack becomes a radial-trace transform in the Fourier $(\mathbf{k}_h, k_z)$ domain with the relationship between angle and radial-traces given by

$$\tan\gamma = -\frac{|\mathbf{k}_h|}{k_z}. \tag{A-10}$$

A simple algorithm for converting offset-domain CIP gathers to the angle domain with equation (A-10) starts by taking the Fourier transform over the depth and offset axes to form gathers in the $(\mathbf{k}_h, k_z)$ domain. Interpolating the energy along radial traces (cones in 3-D seismology) described by equation (A-10) forms gathers in the (γ, k_z) domain. Finally, an inverse Fourier transform along the depth axis produces angle domain gathers that are functions of γ and z.

Sava and Fomel (2000) implement an alternative approach. They begin by defining a linear forward modeling operator that maps angle-domain CIP gathers to the offset domain still based on equation (A-10). To transform gathers from the offset domain to angle domain, they apply the least-squares inverse of this forward operator, which can be computed efficiently with a tridiagonal solver. This has advantages with regard to preserving amplitudes Sava et al., 2001) and was the approach used for the examples in this paper.

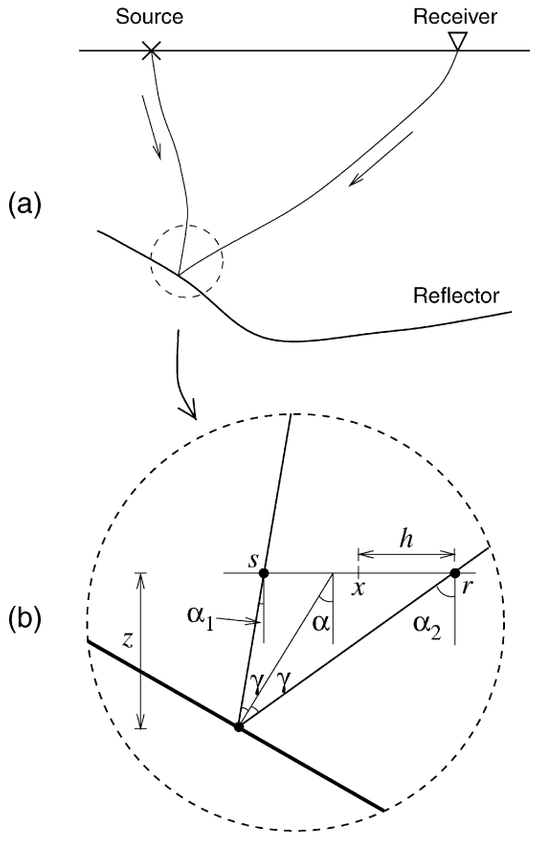

FIG. A-1. Specular energy propagates towards the reflection point as it is downward continued during migration. In general, the velocity of the overburden may be complex (a); however, the velocity should be smooth in the vicinity of the reflection point (b).